SSRG International Journal of Civil Engineering
ISSN: 2348-8352/ https://doi.org/10.14445/23488352/IJCE-V12I2P103

Volume 12 Issue 1, 15-30, February 2025

Original Article

Numerical Investigations on the Dynamic Response of a Long-Span Arch Bridge Under Heavy Truck Loads

Meera Jacob[1], S. Deepa Balakrishnan[2]

[1,2]*Division of Civil Engineering, School of Engineering, Cochin University of Science and Technology, Kochi, Kerala, India.*

[1]*Corresponding Author : meerajacob@cusat.ac.in*

Received: 04 December 2024 Revised: 05 January 2025 Accepted: 06 February 2025 Published: 27 February 2025

Abstract *- Loads of dynamic nature are critical for any bridge structure and must be accurately determined. This paper deals with the dynamic response analysis of a long-span arch bridge due to heavy truck loads under various combinations of vehicle speeds on different road roughness profiles, using numerical modeling and MATLAB coding. Four vehicle loading scenarios were analysed, involving two trucks moving in the same and opposite directions at the same and varying speeds. The dynamic responses in terms of displacement, velocity, and acceleration were computed and compared. The results reveal that the analysed vehicle loading scenario of trucks moving at the same speed in the same direction exhibited a maximum increase of 73%, 104%, and 22% in dynamic responses compared to the other three analysed vehicle loading scenarios. The study also revealed that the roughness of the road surface is a crucial parameter influencing the bridge's dynamic responses. In addition, dynamic amplification factor and pedestrian comfort analysis were also computed for the various vehicle loading scenarios.*

Keywords *- Bridge, MATLAB coding, Quarter-Vehicle Model, Road roughness, Vehicle-bridge interaction.*

1. Introduction

The transportation sector is developing day by day. The advancement in transportation facilities has aided in accessing various remote areas, which has led to their development. Long-span bridges have great importance in the transportation segment. Long-span bridges help to connect distant areas or naturally challenging areas like valleys, gorges, etc., where other transportation facilities cannot be built.

Any bridge with a span greater than 120m can be termed a long-span bridge [1]. Arch bridges may be adopted up to a maximum span of 600m and above 600m; suspension and cable-stayed bridges are then considered. As these structures are highly slender, they are always prone to failure from dynamic loads. The dynamic loads that act on a long-span bridge include pedestrian, vehicle, seismic forces, wind, or combinations of the above-specified loads. Determining the effects of dynamic forces on structures analytically is possible by finite element modeling, which is a critical and powerful analytical tool [2-4].

One of the main factors that contribute to the dynamic loading on bridges is road roughness profiles [5-8]. As for the vehicle loads, vehicle speed and the number of vehicles is important in the response of the structure [5, 7, 9-12]. Further, vehicle type, vehicle weight, number of axles, weight on each axle, and wheelbase are the other major parameters required for the simulation of vehicle loads [13].

To ascertain the true behavior of the bridge under vehicle loading, the road roughness profiles and vehicle loads must be accurately simulated. Road profiles, as per ISO standards, can be artificially generated using MATLAB coding, while the dynamic vehicle loads can be generated using a simple Quarter Vehicle Model (QVM). The major responses of the bridge are derived and evaluated in terms of displacements, velocities, and accelerations [13-18]. It is also important to determine how the dynamic loads magnify the response of structures in comparison with the static loads. This is essential in designing new structures as well as to ensure the safety and reliability of existing structures. This magnification in the dynamic responses of bridges can be computed using dimensionless factors such as the Dynamic Amplification Factor. Further, dynamic loading on bridges generates vibrations, which may affect the comfort level of pedestrians. Excessive vibrations will produce discomfort as well as a sense of fearfulness in pedestrians. In extreme cases, when the loading frequency of vibration matches or is close to the frequency of vibration of the bridge, resonance occurs, which will lead to the collapse of the bridge. Therefore, it is essential to carry out pedestrian comfort analysis of bridges.

Numerous studies have been conducted to ascertain the response of a long-span bridge to vehicle loads with constant vehicle speeds. However, as the real-time loading on the bridge is typically a combination of different speeds rather than constant speed, more insight needs to be given to the

response of the bridge under the combination of different speeds. Also, an extensive amount of work has been carried out in the field of suspension and cable-stayed bridges under dynamic loads. However, a lesser quantum of work has been performed in the field of arch bridges with long spans to determine their response under dynamic loadings.

This study mainly focuses on the determination of dynamic responses of a long-span arch bridge under vehicle loads for different road roughness conditions by considering different road profiles. The vehicle loads considered for the study are standard truckloads, as truckloads are the heaviest among the various classes of vehicles. The study is carried out for a range of constants and combinations of different speeds and directions. Also, dynamic amplification factor and pedestrian comfort analyses were performed for each loading scenario.

2. Methodology

The methodology adopted for the study includes, (i) Formulation of artificial road profiles, (ii) Generation of artificial road profiles, (iii) Analyses Methods, (iv) Dynamic loading of vehicles, (v) Results and discussions, and (vi) Conclusion.

2.1. Formulation of Artificial Road Profiles

Road profiles are described as the variation in the height of the road surface along the length of the road. Road profiles can be either stationary Gaussian or non-stationary Gaussian Road profiles. However, stationary Gaussian Road profiles are extensively used as models for artificial road profile generation [19]. As artificial profiles are used for assessing dynamic loads, stress on vehicles, and passengers' comfort, many studies on the design and analysis of vehicle suspensions are often based on artificial profiles [20]. There are numerous methods for generating artificial profiles, such as the sinusoidal approximation and shaping filter approach, of which the sinusoidal approach, which is based on ISO 8608: 2016 [21], is widely used for theoretical studies due to the simplicity of the method [22, 23].

Artificial road profiles for simulation can be generated following ISO 8608:2016 [15, 21, 24]. ISO 8608:2016 [21] classifies road profiles into 8 classes, class A to H, depending on the Power Spectral Density (PSD) of vertical displacements, G_d, which in turn is a function of spatial frequency, n, and angular spatial frequency, Ω. Table 1 shows the road classification as per ISO 8608:2016 [21]. On comparing the PSDs allied with different classes, it can be perceived that class A has a trivial degree of roughness and can be considered to have a very good surface condition. As we move downward from class A, the degree of roughness increases, namely, class B - good surface, class C - average, class D - poor surface, class E - very poor surface, and classes F to H indicate unpaved surfaces with a higher degree of roughness. ISO 8608:2016 [21] provides fitted PSD of vertical displacements, which can be used to generate artificial road profiles for simulations. As per ISO 8608:2016 [21], the expression for displacement PSD can be given as in Equation (1).

$$G_d(n) = G_d(n_0) \cdot \left(\frac{n}{n_0}\right)^{-w} \quad (1)$$

Where 'w' is the exponent of fitted PSD and n_0 is the conventional value of spatial frequency. The value of the exponent of fitted PSD is specified as 2 for the simulation of artificial surfaces as per ISO 8608:2016 [21], and the equations used for simulating road roughness profiles can be demarcated as given in Equation (2) and Equation (3).

$$G_d(n) = G_d(n_0) \cdot \left(\frac{n}{n_0}\right)^{-2} \quad (2)$$

$$G_d(\Omega) = G_d(\Omega_0) \cdot \left(\frac{\Omega}{\Omega_0}\right)^{-2} \quad (3)$$

Where Ω_0 is the conventional value of angular spatial frequency. The values of G_d (n_0), and G_d (Ω_0) are obtained from Table 1 depending on the required road classes.

Table 1. Road classification as per ISO 8608:2016 [21]

Road Class	G_d (n_0)		G_d (Ω_0)	
	Lower Limit	Upper Limit	Lower Limit	Upper Limit
A	-	32	-	2
B	32	128	2	8
C	128	512	8	32
D	512	2048	32	128
E	2048	8192	128	512
F	8192	32768	512	2048
G	32768	131072	2048	8192
H	131072	-	8192	-

2.2. Generation of Artificial Road Profile

It is feasible to generate an artificial road profile following the ISO classification of road roughness with regard to the PSD of vertical displacement through Fourier Transforms [15]. If a continuous road profile of a definite value of spatial frequency n bounded within a frequency band of Δn is considered, the Power Spectral Density function [15] for a generic spatial frequency value n_i can be expressed as given in Equation (4).

$$G_d(n_i) = \lim_{\Delta n \to 0} \frac{\Psi_x{}^2}{\Delta n} \quad (4)$$

Where Ψ_x is the mean square value of the function within the frequency band of Δn. Further, the road roughness profile can be demarcated in terms of an array of discretized elevations and can be defined using a simple harmonic function [15] as specified in Equation (5).

$$h(x) = A_i \cos(2\pi n_i x + \emptyset \quad (5)$$

Where A_i is the amplitude, n_i is the spatial frequency, and $\emptyset$ is the phase angle. From Equation (4), the mean square value of the harmonic function can be expressed as in Equation (6).

$$\Psi_x{}^2 \quad (6)$$

Previous studies reveal the viability [15, 25] of generating an artificial road roughness profile as per ISO 8608:2016 [21] using the known PSD function of vertical displacements, which can be expressed as in Equation (7).

$$h(x) = \sum_{i=0}^{N} \sqrt{\Delta n}\,.\,2^k.10^{-3}.\frac{n_0}{n_i}.\cos(2\pi n_i x + \emptyset) \quad (7)$$

Where x varies from 0 to the total length (L) of road profile generation. Also, the frequency band, $\Delta n = \frac{1}{L}$ and number of points generated, $N=\frac{L}{B}$; where B is the sampling interval. k is a constant value depending on the ISO 8608:2016 [21] classification of road profiles, and the values are as specified in Table 2.

Table 2. Values of k for ISO 8608:2018 road surface classification [15]

Road Class		k
A	B	3
B	C	4
C	D	5
D	E	6
E	F	7
F	G	8
G	H	9

In this study, road roughness plays a critical role in influencing the dynamic response of the long-span arch bridge. To simulate realistic road conditions, artificial road profiles were generated using MATLAB coding and categorized according to the ISO 8608:2016 road classification standards. These classifications include Class A (Very Smooth), Class C (Semi-Rough), and Class E (Highly Rough), each representing different levels of surface irregularities.

Class A roads are characterized by minimal undulations, with displacement variations limited to ±3 mm, ensuring a smooth driving experience. Class C roads feature moderate irregularities, with displacement variations reaching ±16 mm, creating a semi-rough surface. Lastly, Class E roads have significant surface irregularities, with displacement variations of up to ±60 mm, creating a highly rough road surface.

Each of these road profiles was generated using a Fourier transform approach, which enables the simulation of realistic and varied road surfaces. By incorporating these different profiles, the study examines how road roughness affects the bridge's dynamic behavior. The impact of these varying surface conditions on the bridge's response is assessed by evaluating the structure's performance under each road classification, providing a comprehensive understanding of how road irregularities influence the overall bridge dynamics and vehicle interaction. MATLAB codes were developed to generate road profiles for a total length of 216 m, which is the total length of the bridge considered for the study. Additionally, the randomness of the road profile was taken into consideration to minimize the underestimation or overestimation of dynamic loads in simulation. Figure 1 shows the road profiles generated for very smooth, semi-rough, and highly rough surfaces.

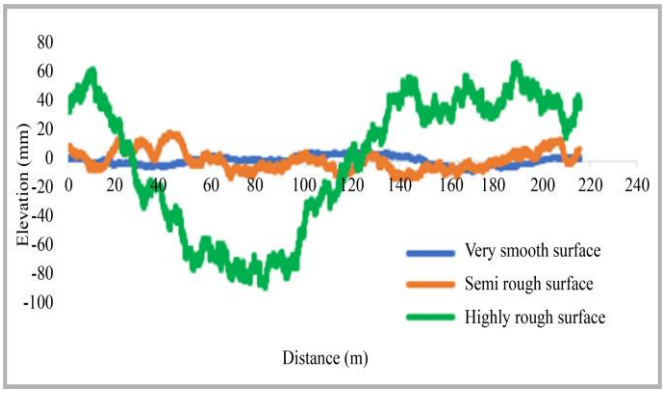

Fig. 1 Artificial road profiles generated for very smooth, semi-rough, and highly rough surfaces

The road profile generated using MATLAB coding is in terms of vertical displacements (elevations) in mm for the total length (distance) of the bridge. From Figure 1, it is observed that the roughness of the very smooth road profile varies between +3 mm to -6 mm, the roughness of the semi-rough road profile varies between +16 mm to -11 mm, and that of the highly rough road profile varies between +60 mm to -80 mm.

Random multiple iterations have been carried out to generate the above-specified road roughness profiles. The value of road roughness obtained in the present study is on par with the values reported in the published literature, thus validating the reliability of the results [15, 26-28].

2.3. Analyses Methods

The analysis methods adopted for the study involve the development of the vehicle model and FE model of the bridge considered for the study, followed by the formulation of vehicle-bridge interaction equations.

2.3.1. Vehicle Model

When a vehicle passes over uneven surfaces, it causes vibrations, which in turn affects the loads acting on it. The load generated due to the movement of a vehicle is not constant and is a function of space and time. Further, the load generated depends on the vehicle type, vehicle weight, speed

of vehicle, suspension type of vehicle, surface unevenness, etc. The vehicle considered for the present study is a single-unit truck [29]. The vehicle consists of two axles. It has 7 degrees of freedom, including vertical displacement of the wheels, the vertical displacement, pitch angle displacement, and lateral inclination displacement of the vehicle, as shown in Figure 2(a). In Figure 2(a), m_v is the mass of the vehicle, k_{s1} to k_{s4}, and c_{s1} to c_{s4} is the stiffness and damping of the vehicle body (sprung mass), while m_{u1} to m_{u4} and k_{u1} to k_{u4} is the tire (unsprung mass) mass and stiffness. The most common method of simulating a vehicle-surface interaction is the linear Quarter-Vehicle Model (QVM), or in the present context, the linear quarter-truck model. The linear quarter-truck model is developed from the equations of motion, which include the mass of the vehicle, suspension stiffness, tire stiffness, and damping of suspension.

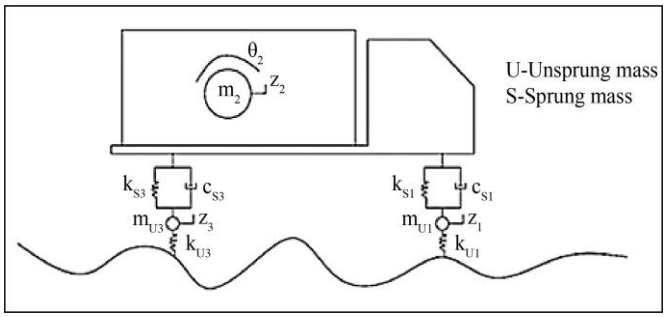

Fig. 2(a) Vehicle elevation

For the development of the model, it is assumed that the tire of the truck is modeled as a spring without damping, and it is always in contact with the road surface. Further, the rotational motion of the wheel and body is neglected [30]. This model can be effectively used for perusing the interaction between the vehicle and the road surface. However, there are certain limitations for the linear QVM, which include: (1) It does not depict the geometric effects of the full car model, and (2) The assumption of constant contact of the tire with the road surface may not hold true in all the cases [30].

Due to the assumptions and limitations of the model, the dynamic responses obtained from the study may be slightly higher than the actual responses. Figure 2(b) represents a schematic representation of the linear quarter-truck model considered for the study. The various vehicle characteristics of the truck used for developing the linear quarter-truck model are tabulated in Table 3. In this study, the Quarter Vehicle Model (QVM) is utilized to simulate the dynamic response of the long-span arch bridge under truck loads. The QVM parameters selected for the vehicle model are designed to represent typical characteristics of a heavy truck. The sprung mass, which refers to the portion of the vehicle's mass supported by the suspension system, is set at 4500 kg. This value corresponds to the mass of the vehicle's body, including the cargo and frame, that is isolated from the road surface by the suspension system. The unsprung mass, which represents the mass of components that are not supported by the suspension (such as the wheels, tires, and axles), is 650 kg. The suspension system, responsible for absorbing road irregularities and reducing vibrations transmitted to the vehicle body, has a stiffness of 570,000 N/m. This high stiffness value indicates a firm suspension setup. The damping coefficient of the suspension is 21,000 Ns/m, representing the resistance to motion and the rate at which the suspension dissipates energy to control oscillations. Finally, the tire stiffness, which models the tire's resistance to compression as it interacts with the road surface, is set at 3,000,000 N/m. These parameters are crucial for accurately simulating the vehicle's behavior as it moves over the bridge and interacts with different road roughness profiles.

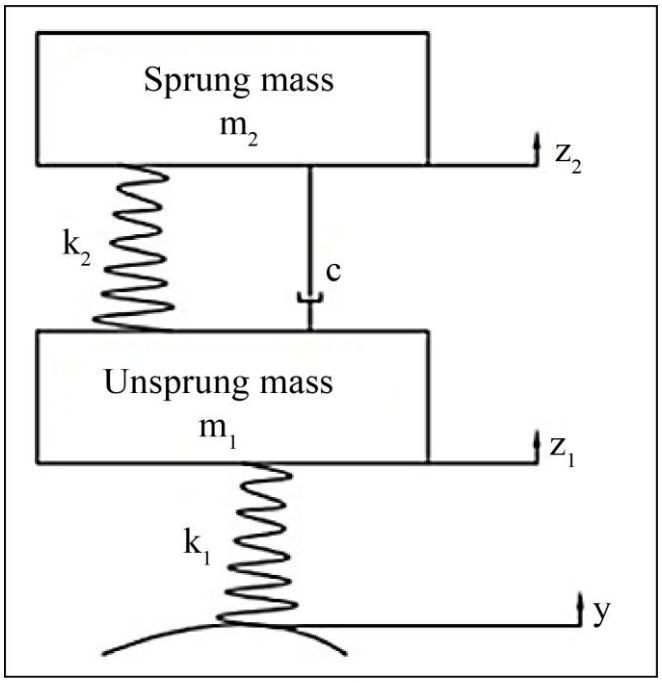

Fig. 2(b) Schematic representation of the linear quarter truck model

Table 3. Vehicle characteristics [15]

Vehicle Characteristics	Truck
Unsprung mass, m_1 [kg]	650
Sprung mass, m_2 [kg]	4500
Suspension stiffness, k_2 [N/m]	570000
Suspension damping, c [Ns/m]	21000
Tire stiffness, k_1 [N/m]	3000000

Regarding the linear quarter truck model, the equations of motion can be written as specified in Equation (8) and Equation (9).

$$m_2\ddot{z_2} + c\,(\dot{z_2} - \dot{z_1}) + k_1(z_2 - z_1) = 0 \qquad (8)$$

$$m_1\ddot{z_1} + c\,(\dot{z_1} - \dot{z_2}) + k_1(z_1 - z_2) - k_2(z_1 - y) = 0 \qquad (9)$$

The dynamic load generated due to the vehicle-surface interaction depends on all the above-specified vehicle

characteristics. However, the variation of dynamic load generated along the road profile is calculated by the stiffness of unsprung mass, k_2, elevation of roughness, y, and the relative displacement between the unsprung mass and road roughness profile, z_1. Further, the total wheel load of the vehicle is calculated as the sum of the static load and the dynamic load.

2.3.2. Three-Dimensional FEM Model of Long-Span Bridge

In the present study, a three-dimensional finite element model of a real-time bridge, the Cetina bridge, was developed to perform vehicle bridge interaction studies. The Cetina Bridge is a long-span open spandrel deck-type arch bridge spanning across the Cetina River Canyon near Trilij in Croatia [31]. The arch portion of the bridge has a length of 140.3m with a span-to-rise ratio of 1:6.8, which supports 10 spans of deck, each of 21.6m. The bridge's longest span, including the arch, is 151.2 meters long, and the total length of the bridge is 216m. The overall width of the bridge is 10.5m, including the two-lane traffic, sidewalks, and kerbs. The bridge's superstructure consists of five precast prestressed T-girders spaced at a distance of 1.9m center-to-center supporting cast-insitu deck slab. Further, the arch is connected to the deck through nine pairs of spandrel columns. The deck slab, T-girders, and arch are of concrete grade C45/55, which has a compressive strength of 45MPa, while the spandrel columns are of concrete grade C30/37, which has a compressive strength of 30MPa. In the FE modeling of the bridge, the T-girders are modeled using BEAM elements, the deck slab is modeled using PLATE/SHELL elements, and the arch and columns are modeled using SOLID elements. The finite element model of the long-span bridge developed on midas Civil 2023 (v1.1) consists of 11961 nodes and 8280 elements.

The details for the model development were adopted from the literature [32]. Figure 3 shows the finite element model of the long-span arch bridge. It is essential to perform a modal analysis prior to dynamic loading to determine the mode shapes and period of the structure. Therefore, before the application of dynamic load, the mode shapes and period of the structure were determined using eigenvalue analysis. The period of vibration of the bridge is given in Table 4, and the predominant modes in respective directions are specified in Figure 4.

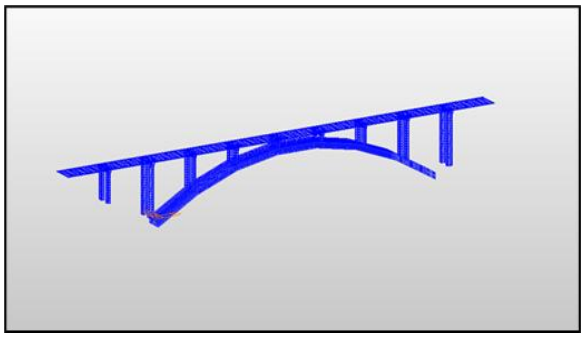

Fig. 3 FE model of the bridge

Table 4. Period of vibration

Mode	Period (seconds)	Mode	Period (seconds)
1	0.892	7	0.292
2	0.782	8	0.240
3	0.407	9	0.199
4	0.385	10	0.181
5	0.378	11	0.173
6	0.299	12	0.158

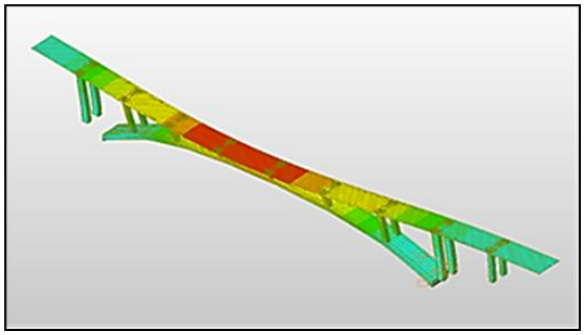

Fig. 4(a) Mode 1 - along the transverse direction

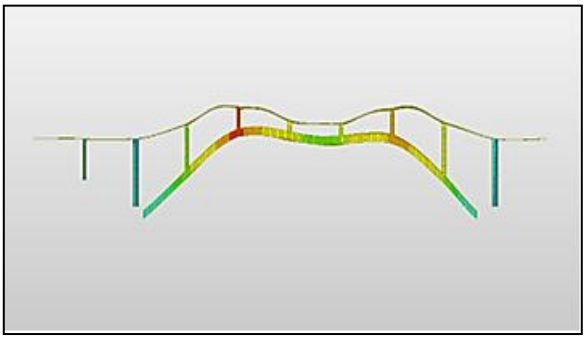

Fig. 4(b) Mode 7 - along the vertical direction

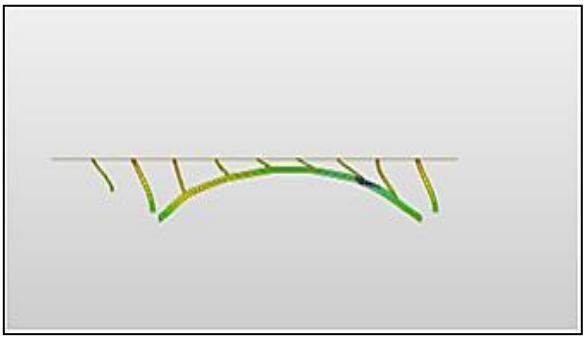

Fig. 4(c) Mode 6 – along the longitudinal direction

2.3.3. Formulation of Vehicle-Bridge Interaction Equations

On developing the mechanical model of the vehicle and bridge systems, it is essential to formulate the vibrational differential equations of the vehicle-bridge interaction system, which may be solved by coupling the two subsystems through coordinate conditions of force and displacement. The vibration differential equation for the vehicle system and bridge can be written in Equation (10) and Equation (11).

$$m_v\ddot{x}_v(t) + c_v\dot{x}_v(t) + k_v x(t) = F_v(t) \quad (10)$$

$$mb\ddot{y}b(t) + cb\dot{y}b(t) + kbyb(t) = Pb(t) \quad (11)$$

Where $m_{v/b}$, $c_{v/b}$, and $k_{v/b}$ are the mass, damping, and stiffness matrices of the vehicle and bridge, respectively. $\ddot{x}_v(t)$, $\dot{x}_v(t)$, $x_v(t)$ and $\ddot{y}_b(t)$, $\dot{y}_b(t)$, $y_b(t)$ are the acceleration, velocity, and displacement of the vehicle and bridge respectively. $F_v(t)$ is the load vector of the vehicle, while $P_b(t)$ is the bridge's equivalent nodal vector. The displacement and force at the contact points between the vehicle's wheels and the bridge affect the dynamic interaction between the two systems. However, vehicle bridge interaction studies are based on several assumptions regarding the interactive effects between the bridge and the wheels of the vehicle, which are as follows:

The tires of the vehicle are in continuous contact with the bridge deck, and the relative vertical displacement vector can be defined in Equation (12).

$$\Delta Z(t) = Z_b(t) - Z_v(t) + h(x) \quad (12)$$

Where $Z_b(t)$ and $Z_v(t)$ are the vertical displacement vector of the bridge and vehicle, respectively, and h(x) is the vector value of the road surface roughness profile at the contact point. The interactive force between the vehicle tire and bridge at the contact surface obeys D'Alembert's principle, which can be defined in Equation (13).

$$P_b(t) = -P_v(t) = C_w\Delta\dot{Z}(t) + K_w\Delta\dot{Z}(t) \quad (13)$$

Where Pb(t) is the force vector applied onto the bridge by the vehicle and Pv(t) is the force vector applied to the vehicle by the bridge and these force vectors are acting opposite to each other. C_w and K_w are the damping and stiffness matrices of the vehicle. $\Delta\dot{Z}(t)$ is the relative vertical velocity vector of the bridge to the vehicle. There are numerous methods adopted for determining the solution of differential equation of vehicle bridge interaction systems, such as the Wilson-θ method, the central difference method, the piece-wise analytical method, and the Newmark-β method [33]. In the present study, by developing the bridge and vehicle models and given the initial conditions of the vehicle and bridge, the vehicle bridge coupling vibration equations were iteratively solved using the midas Civil 2023(v1.1) platform. The iterative simulation was implemented by constant Newmark-β method with 0.1 seconds time increment and 5% damping ratio.

2.4. Dynamic Loading of Vehicles

The bridge, with a total width of 10.5m (including crash barriers and kerbs), accommodates two lanes as per IRC 6:2017 [34]. Among various vehicle types, trucks are considered the heaviest, so the study focuses on single-unit trucks according to AASHTO standards [29]. For the two-lane configuration, one truck is assigned to each lane, as per the vehicle load distribution. The simulations were designed to examine different loading scenarios involving truck movement. These scenarios include (1) Two trucks moving parallel at the same constant speed (ranging from 40 kmph to 120 kmph), (2) Two trucks moving toward each other at the same constant speed, (3) One truck moving at a constant speed of 60 kmph while the other varies between 40–120 kmph in the same direction, and (4) One truck moving at a constant speed of 60 kmph while the other varies between 40–120 kmph in the opposite directions. The truck models used were in accordance with AASHTO's legal load configurations [29], which define axle loads, spacing, and weight distributions, ensuring the simulation mimics real-world conditions. A total of 30 simulations were performed for constant speed conditions, where the trucks moved at the same speed in both the same and opposite directions across three different road roughness profiles. The constant speeds considered were 40, 60, 80, 100, and 120 kmph. Additionally, 24 simulations were conducted with trucks at varying speeds in the same and opposite directions. Speed combinations included 60-40 kmph, 60-80 kmph, 60-100 kmph, and 60-120 kmph, with the truck in the left lane maintaining a constant speed of 60 kmph while the right lane truck speed varied. The vehicle loads were applied as dynamic nodal loads through force-time functions, and the resulting vertical displacements, velocities, and accelerations of the bridge structure were analyzed.

3. Results and Discussions

The displacement, velocity, and acceleration are the most important responses of a structure to dynamic loads. In this study, the structure's response is assessed in terms of vertical accelerations, vertical velocities, and vertical displacements. In addition, this section discusses the impact of different vehicle factors and road roughness profiles on the bridge's dynamic response. Computation and comparison of dynamic amplification factor and pedestrian comfort analyses for various loading scenarios are also discussed in detail.

3.1. Effect of Vehicle Speed on the Dynamic Response of the Bridge

In the present case, two trucks moving at the same speed and a combination of different speeds in the same direction are considered. For the numerical study, speeds of 40, 60, 80, 100, and 120 kmph are considered for trucks with the same speed, while 60-40 kmph, 60-80 kmph, 60-100 kmph, and 60-120 kmph are considered for trucks with the combination of different speeds, considering 60 kmph as an average speed of the truck. The numerical analyses for the combination of different speeds were carried out in such a way that the speed of 60 kmph was kept constant along the left lane, and the speed in the right lane was varied in each case of simulation. Depending on the respective speed, the force-time function for each wheel load was calculated and inputted. The responses of the structure are extracted and presented in terms of dynamic responses versus locations along the total length of the bridge (x/L). Figures 5(a), 5(c), and 5(e) represent the vertical displacement, vertical velocity, and vertical acceleration of

trucks moving at the same speed in the same direction on a very good road roughness profile. Figures 5(b), 5(d), and 5(f) represent the vertical displacement, vertical velocity, and vertical acceleration of trucks moving at a combination of different speeds in the same direction on a very good road roughness profile. From the plots, it can be shown that for trucks moving at the same speed, the dynamic responses of the bridge increase from 40kmph to 80kmph and reduce at 100 kmph and 120 kmph. This is because the time taken by the vehicle moving at speeds of 100kmph and 120kmph to travel across the whole length of the bridge is 6 seconds and 7 seconds, respectively, which may not be sufficient enough to produce higher dynamic responses on the long-span bridge [35]. Similarly, for the trucks moving at a combination of different speeds, the speed combination of 60-80 kmph resulted in a higher value of dynamic responses than other combinations.

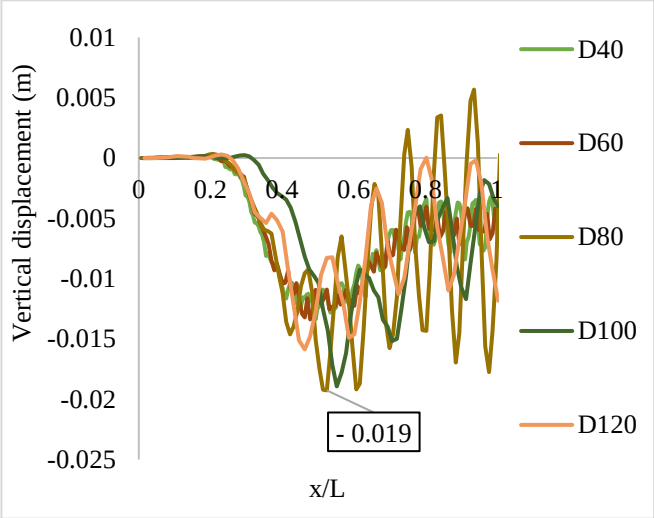

Fig. 5(a) Displacement response of bridge - trucks moving at the same speed in the same direction

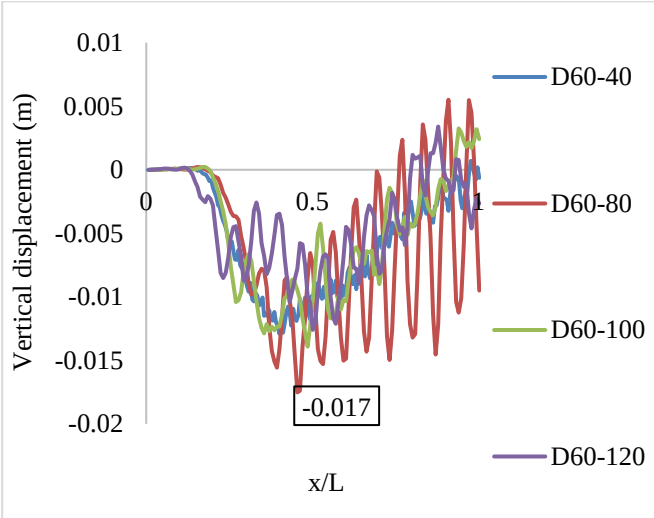

Fig. 5(b) Displacement response of bridge - trucks moving at a combination of different speeds in the same direction

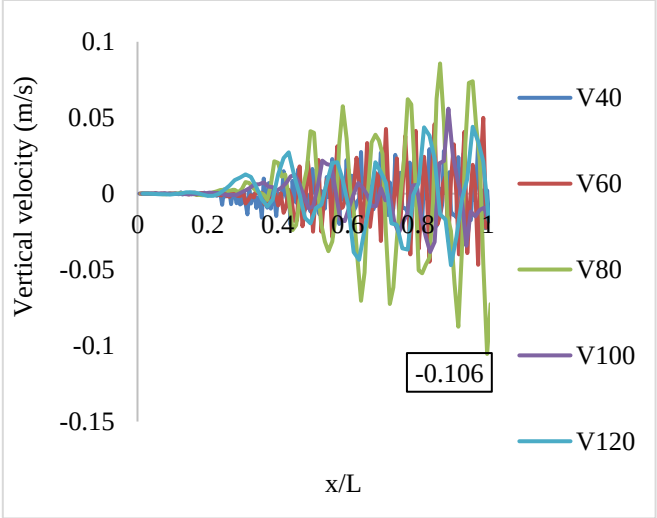

Fig. 5(c) Velocity response of bridge - trucks moving at the same speed in the same direction

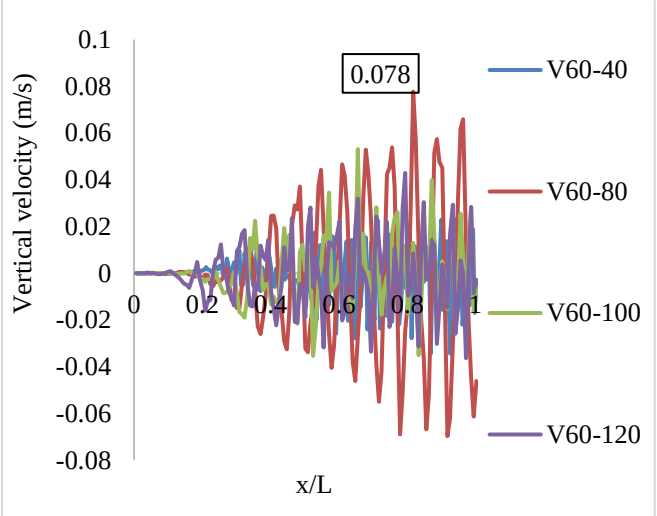

Fig. 5(d) Velocity response of bridge - trucks moving at a combination of different speeds in the same direction

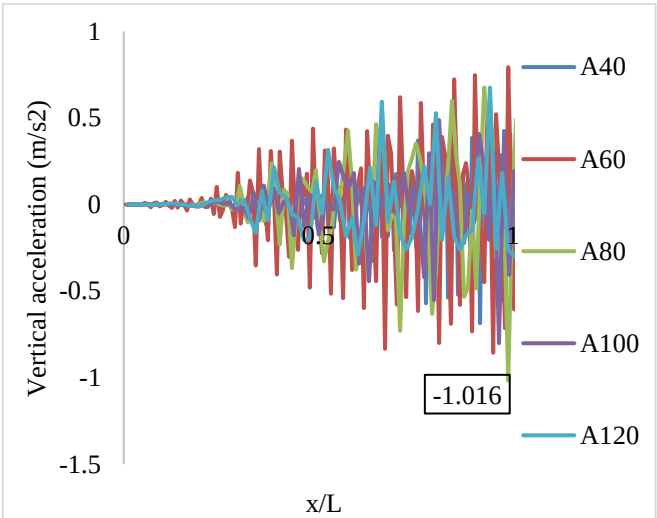

Fig. 5(e) Acceleration response of bridge - trucks moving at the same speed in the same direction

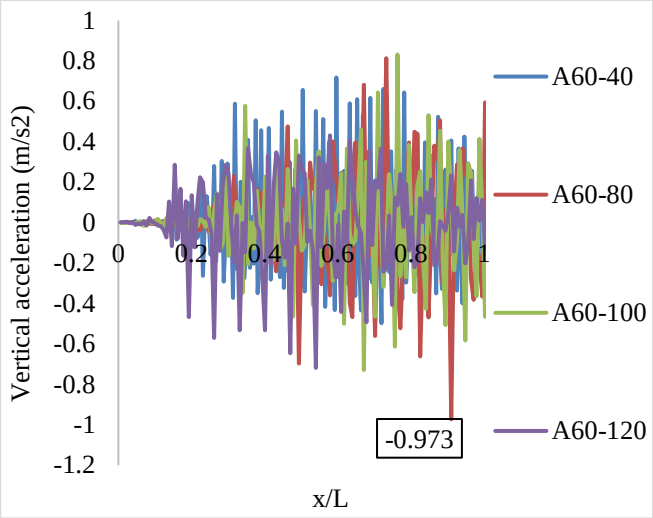

Fig. 5(f) Acceleration response of bridge - trucks moving at a combination of different speeds in the same direction

This is because the crossing time on the bridge for vehicle speeds, 60 and 80 kmph is comparable to any other combination of different speeds. Thus, it can be concluded that the vehicle speed has a considerable effect on the dynamic response of the bridge but it does not vary linearly, as they may depend on many factors other than the speed of the vehicle [37].

Nevertheless, it can be perceived that the dynamic responses of trucks moving at the same speed in the same direction increased by 12% in displacement responses, 36% in velocity responses, and 4% in acceleration responses compared to the dynamic responses of trucks moving at a combination of different speeds in the same direction.

3.2. Effect of Direction of the Vehicle on the Dynamic Response of the Bridge

In the present case, two trucks moving at the same speed in the same direction and in opposite directions are considered. Various speeds considered for numerical analyses are 40, 60, 80, 100, and 120 kmph. For each case of numerical analyses, the wheel load of the truck for the corresponding speed was calculated and inputted as time history functions.

The dynamic response of the structure in terms of vertical displacement, vertical velocity, and vertical acceleration was extracted and reported in terms of dynamic responses versus locations along the total length of the bridge (x/L).

Figures 6(a), 6(b) and 6(c) represent the vertical displacement, vertical velocity, and vertical acceleration responses of the bridge under the trucks moving with the same speed in opposite directions on a very good road roughness profile. On comparing the results with Figures 5(a), 5(c), and 5(e), it can be perceived that similar to trucks moving in the same direction, the dynamic responses of trucks moving in opposite directions also showed a higher value for 80 kmph.

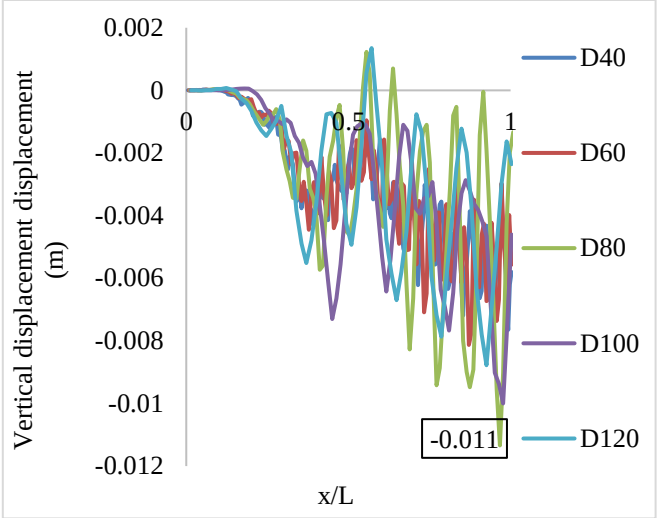

Fig. 6(a) Displacement response of bridge - trucks moving at the same speed in opposite directions

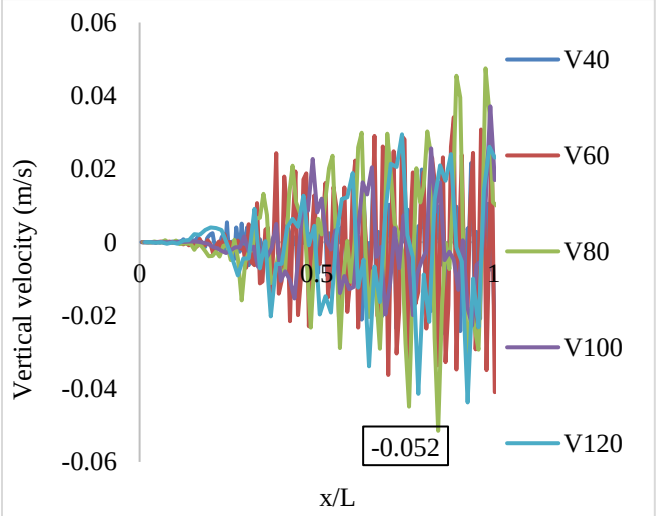

Fig. 6(b) Velocity response of bridge - trucks moving at the same speed in opposite directions

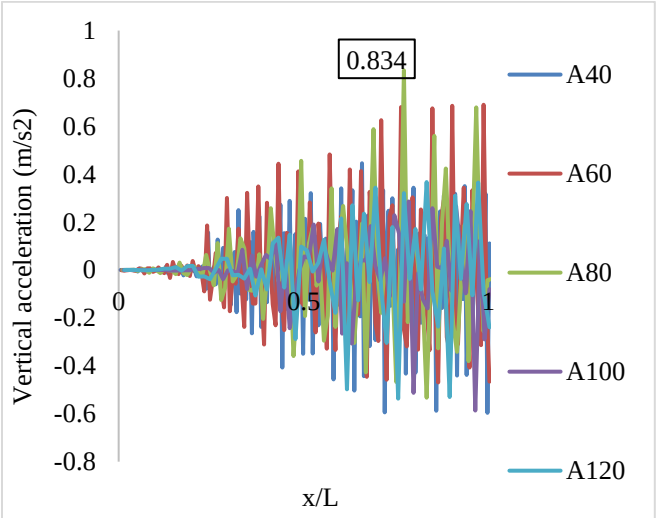

Fig. 6(c) Acceleration response of bridge - trucks moving at the same speed in opposite directions

However, the dynamic responses of trucks moving at the same speed in the same direction increased by 73% in displacement responses, 104% in velocity responses, and 22% in acceleration responses compared to the dynamic responses of trucks moving at the same speed in the opposite directions. This illustrates that the direction of movement of the vehicle is important in the dynamic response of the bridge. A set of numerical analyses was also carried out to evaluate the dynamic response of the bridge under the condition of the trucks moving at a combination of different speeds in opposite directions. Further, the responses were compared with those obtained from trucks moving at the same speed in the same direction. Figures 7(a), 7(b) and 7(c) represent the vertical displacement, vertical velocity, and vertical acceleration of the bridge under the trucks moving at a combination of different speeds in opposite directions on a very smooth road profile condition.

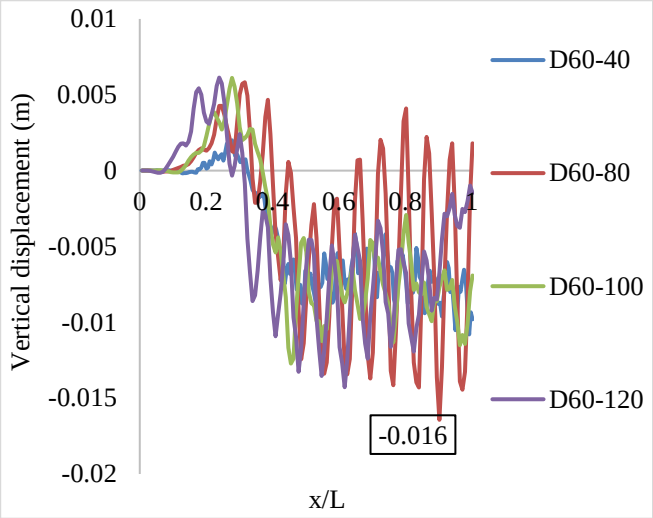

Fig. 7 (a) Displacement response of bridge – trucks moving at a combination of different speeds in opposite directions

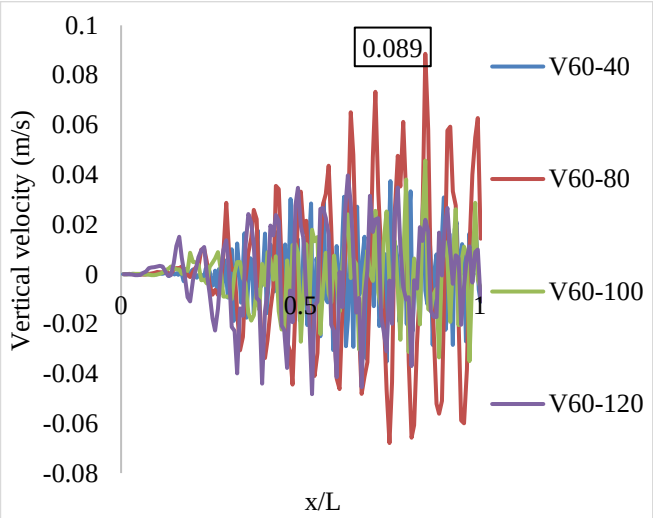

Fig. 7(b) Velocity response of bridge – trucks moving at a combination of different speeds in opposite directions

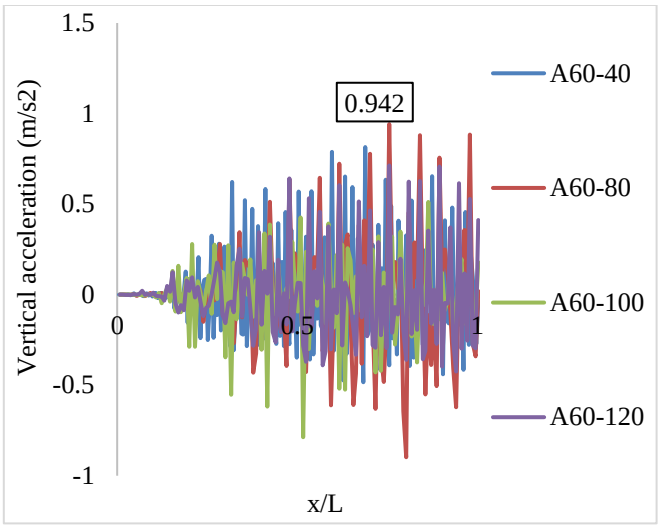

Fig. 7(c) Acceleration response of bridge – trucks moving at a combination of different speeds in opposite directions

On comparing the results with Figures 5(a), 5(c), and 5(e), it can be shown that dynamic responses were similar in such a way that the maximum response was obtained at 80kmph for the same speed and combination of different speeds. Also, the dynamic responses of trucks moving at the same speed in the same direction increased by 19% in displacement responses, 19% in velocity responses, and 8% in acceleration responses compared to the dynamic responses of trucks moving at combination of different speeds in opposite directions.

Also, it can be observed from comparing the displacement responses that, unlike trucks traveling in the same direction, trucks traveling in opposition to one another can have their maximum displacement occur on any span of the bridge, not just the midspan.

3.3. Effect of Surface Roughness on the Dynamic Response of Bridges

The present study considers three surfaces, namely, very smooth road profile, semi-rough road profile, and highly rough road profile. Numerical investigations were conducted for trucks moving at the same speed in the same direction and opposite directions, as well as the combination of different speeds in the same and opposite directions, considering all three road roughness profiles.

For a better understanding of results, only acceleration responses of the long-span bridge under vehicle loads are presented. Figures 8(a), 8(b), 8(c), and 8(d) show the variation of vertical acceleration responses of the bridge for very good road profile, semi-rough road profile, and highly rough road profile for trucks moving at the same speed in the same direction, trucks moving at the same speed in opposite directions, trucks moving at a combination of different speeds in same direction and trucks moving at a combination of different speeds in opposite directions respectively. From the

plots, it can be shown that as the roughness of the road surface increases, the acceleration response of the bridge also increases [18, 36, 37]. For trucks moving at the same speed in the same direction, the acceleration responses are 22% and 58% higher for semi-rough and highly rough road profiles, respectively, when compared with very smooth road profiles.

Also, acceleration responses for trucks moving at the same speed in opposite directions are 12% and 62% higher for semi-rough and highly rough road profiles, respectively, when compared with very smooth road profiles.

Furthermore, the results show that the acceleration responses of trucks moving at a combination of different speeds in the same direction are 13% higher for the semi-rough road profile and 57% higher for the highly rough road profile compared to the very smooth road profile.

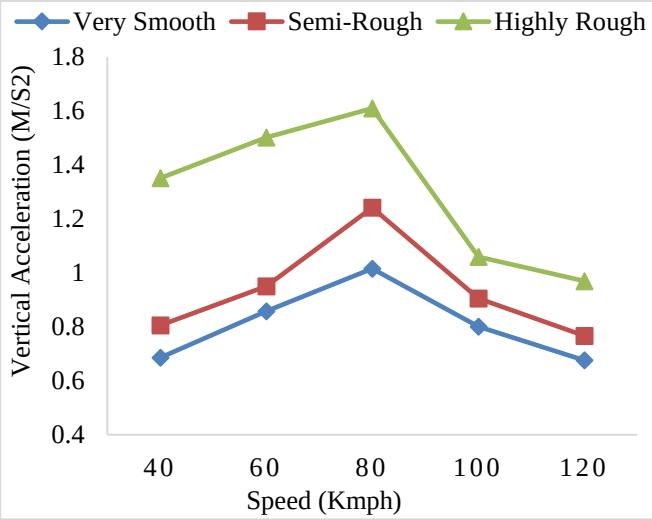

Fig. 8(a) Acceleration response – trucks moving at the same speed in the same direction

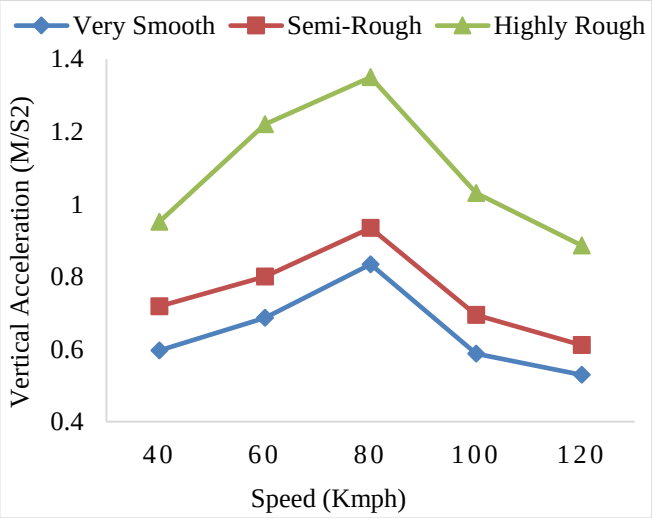

Fig. 8(b) Acceleration response – trucks moving at the same speed in opposite directions

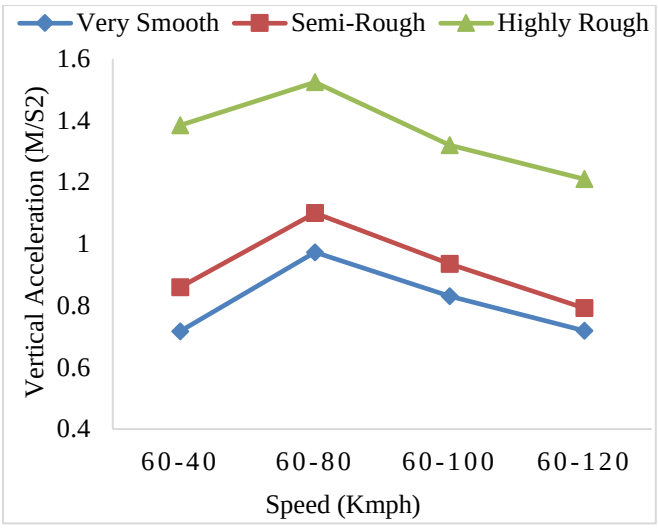

Fig. 8(c) Acceleration response – trucks moving at a combination of different speeds in the same direction

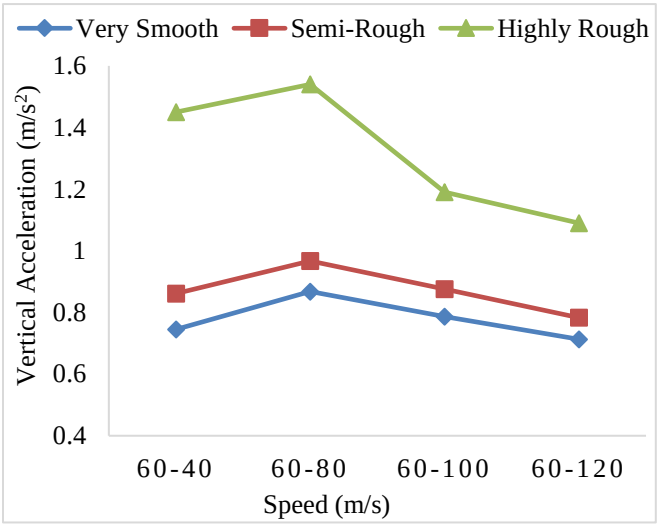

Fig. 8(d) Acceleration response – trucks moving at a combination of different speeds in opposite directions

Similarly, for trucks moving at a combination of different speeds in opposite directions, acceleration responses exhibited an 11% and 77% increase than that of very smooth road profile for semi-rough road profile and highly rough road profile respectively. A similar trend of results has been obtained in the case of displacement and velocity responses of the bridge. The increase in the dynamic response of the bridge is because the increase in the degree of roughness of the road profile contributes to increased dynamic loading on the structure.

3.4. Dynamic Amplification Factor

Dynamic Amplification Factor (DAF) is an important parameter that characterizes the effect of dynamic loading on a bridge. The dynamic amplification factor is generally expressed as the ratio of the dynamic response to the static response of the bridge. Thus, it can be described as in Equation (14).

$$DAF = \frac{Q_{dynamic}}{Q_{static}} \quad (14)$$

Where $Q_{dynamic}$ Q_{static} are dynamic and static displacements at the midspan of the bridge. This parameter summarizes how the response of the bridge is amplified in the event of dynamic loading. In the present study, DAF has been determined for each of the four scenarios, including trucks moving at the same speed in the same direction and opposite directions and trucks moving at a combination of different speeds in the same and opposite directions. Furthermore, DAF was computed for each of the three road roughness profiles. Figures 9(a) and 9(b) depict the plot of the dynamic amplification factors for trucks moving at the same speed and a combination of different speeds in the same direction and opposite directions. For a better understanding of the results, only the plots of DAF for very smooth road surface roughness profiles are presented.

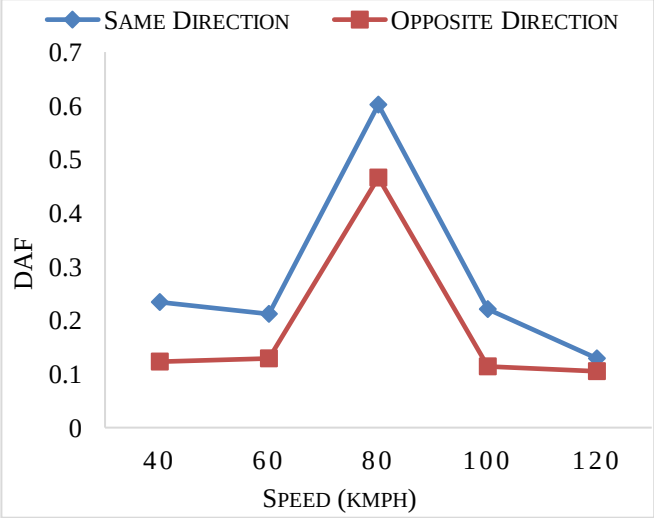

Fig. 9(a) DAF for trucks moving with the same speed on a very smooth road roughness profile

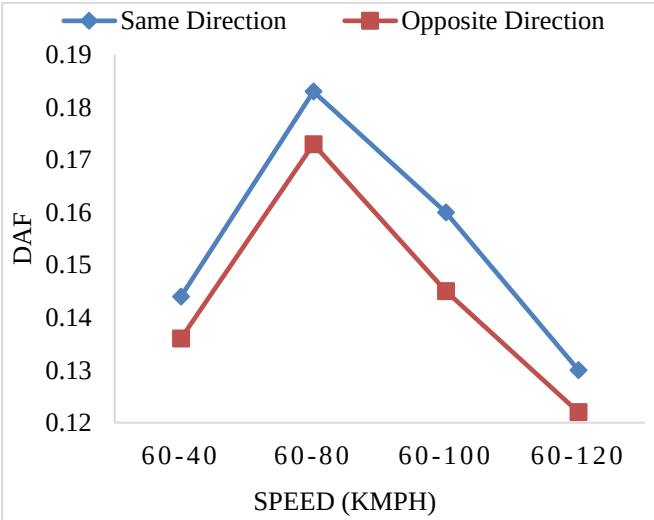

Fig. 9(b) DAF of trucks moving with a combination of different speeds on a very smooth road roughness profile

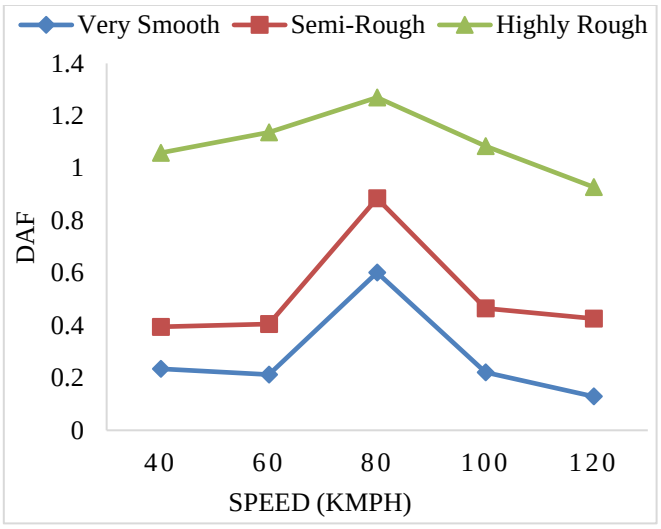

Fig. 9(c) DAF for trucks moving with the same speed in the same direction for three different road roughness profiles

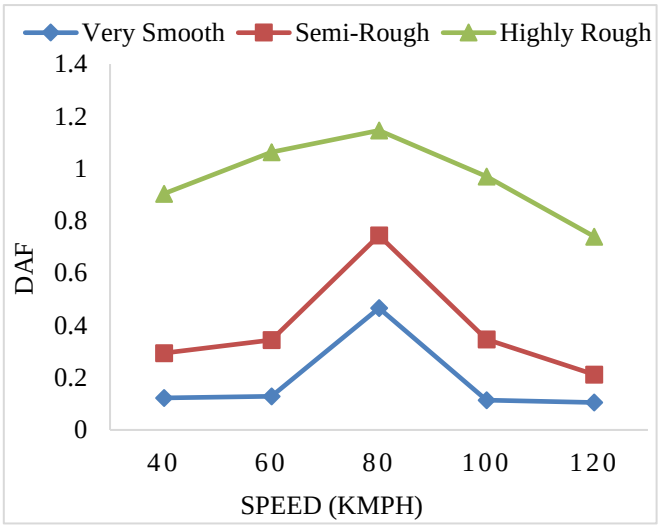

Fig. 9(d) DAF for trucks moving with the same speed in opposite directions for three different road roughness profiles

From Figures 9(a) and 9(b), it can be shown that for trucks moving at the same speed, DAF for 80kmph has resulted in maximum value for both the same and opposite directions. Similarly, for trucks moving with a combination of different speeds, the combination of 60-80kmph has resulted in a maximum value of DAF for both the same and opposite directions. A similar trend of results has been obtained for semi-rough road profiles and highly rough road profiles. Figures 9(c) and 9(d) show the variation of DAF for trucks moving at the same speed in both the same and opposite directions for three different road surface roughness conditions. DAF for trucks moving at the same speed in the same direction is 32% and 53% higher than that of a very smooth road profile for semi-rough and highly rough road profiles, respectively. Similarly, DAF for trucks moving in opposite directions is 38% and 60% higher than that of a very smooth road profile for semi-rough and highly rough road profiles, respectively.

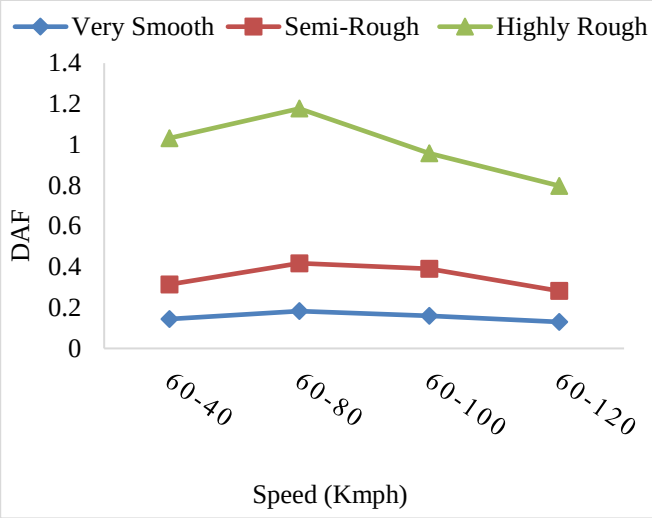

Fig. 9(e) DAF for trucks moving with a combination of different speeds in the same direction for three different road roughness profiles

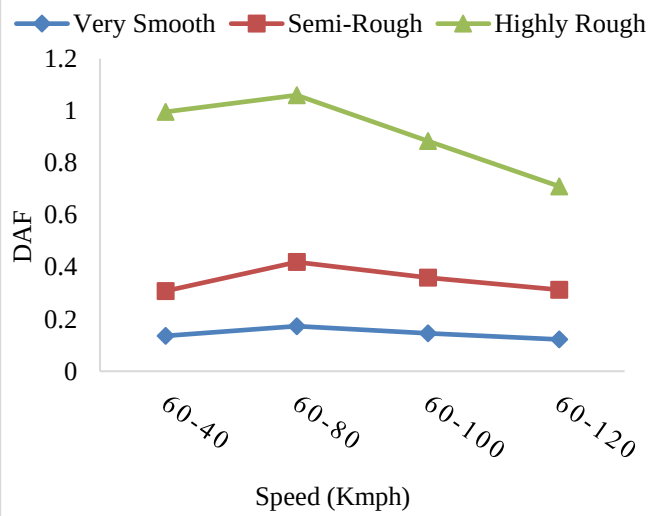

Fig. 9(f) DAF for trucks moving with a combination of different speeds in opposite directions for three different road roughness profiles

Figures 9(e) and 9(f) show the variation of DAF for trucks moving with a combination of different speeds in both the same and opposite directions for three different road surface roughness conditions. The DAF for trucks moving with a combination of different speeds in the same direction is 3 times and 7 times higher than that of a very smooth road profile for semi-rough and highly rough road profiles, respectively. Similarly, DAF for trucks moving with a combination of different speeds in opposite directions is 3 times and 6 times higher than that of a very smooth road profile for semi-rough and highly rough road profiles, respectively. It can be perceived from the above results that as the degree of road roughness increases, the dynamic amplification factor also increases.

3.5. Comfort Analysis

When vehicles move over a bridge, it undergoes vibrations. These vibrations may be experienced by pedestrians on the bridge, affecting their comfort. Several indices are used to express the effect of the vibrations of the bridge deck due to vehicle loads on the level of comfort experienced by the pedestrians on the bridge. The present study considered the Dieckmann Index, K, to determine the vibrational effect of the bridge on human body comfort. The Dieckmann index is calculated considering the frequency and amplitude of vibrations generated when the vehicle moves over the bridge. Table 5 shows the calculation value of the Dieckmann Index when a bridge vibrates vertically [36].

Table 5. Dieckmann index calculation depending on the frequency of vibration of the bridge [36]

Frequency (f)	Dieckmann Index (K)
f < 5Hz	$K = Df^2$
5Hz<f<40Hz	K = Df
f > 40Hz	K = 200D

Table 6. Indication of pedestrian comfort level based on Dieckmann index [36]

K	Human Feeling of Vibration
0.1	Can feel the vibration
1	Can tolerate any long-time vibration
10	Can tolerate short-time vibration
100	Cannot tolerate vibration

Where D and f are the amplitude and frequency of vibration, respectively. According to the value of K, the comfort level of the human body in the event of bridge vibration is tabulated in Table 6 [36]. Based on the displacement time history results, the variation of the Dieckmann index for trucks moving at the same speed in the same direction and opposite directions was calculated. Similarly, the Dieckmann index for trucks moving with a combination of different speeds in the same direction and opposite directions was also computed. Figures 10(a) and 10b show the plots of variation of the Dieckmann index for the above-specified scenarios for a very smooth road roughness profile. As can be seen from the results, when trucks are moving at the same speed in the same and opposite directions, K for 40 and 60 kmph is well below 0.1, indicating that the human body does not feel the vibrations. However, when trucks are traveling at 80 to 120 kmph, the vibrations can be felt by the human body, as indicated by the Dieckmann index values specified in Table 6. For trucks moving with a combination of different speeds, except for the 60-120 kmph combination in opposite directions, all the other combinations, in both the same and opposite directions, resulted in values above 0.1, which indicates that the vibrations generated can be felt by the human body. Figures 10(c) to 10f show the variation of the Dieckmann index for different degrees of road surface roughness profile for trucks moving at the same speed and with a combination of the different speeds in both the same and opposite directions. It can be seen from the plots that as the degree of road roughness increases, the Dieckmann index also increases. However, the index values show that the vibrations produced in all the cases fall under category 1, “can feel the vibration”.

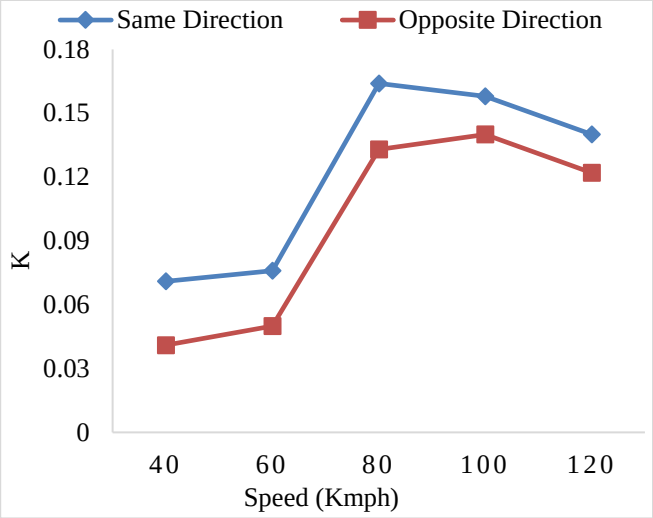

Fig. 10(a) Dieckmann index for trucks moving at the same speed on very smooth road roughness profile

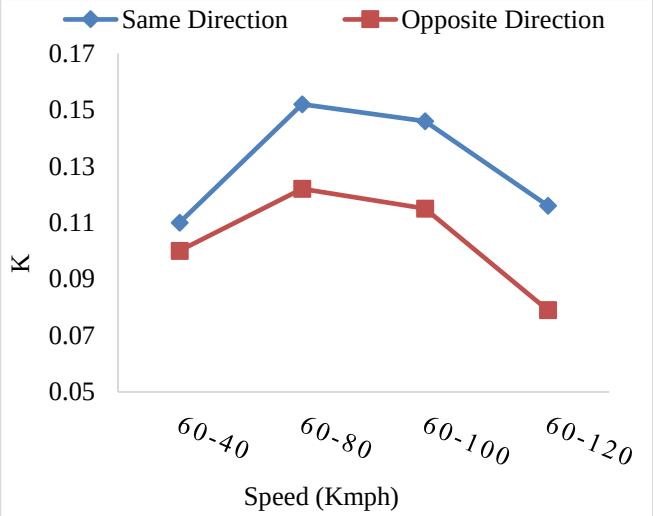

Fig. 10(b) Dieckmann index for trucks moving with a combination of different speeds on very smooth road roughness profile

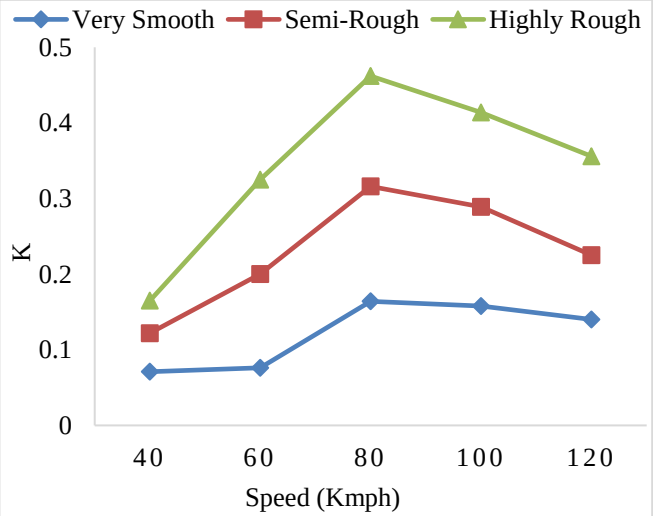

Fig. 10(c) Dieckmann index for trucks moving at the same speed in the same direction for different road roughness profiles

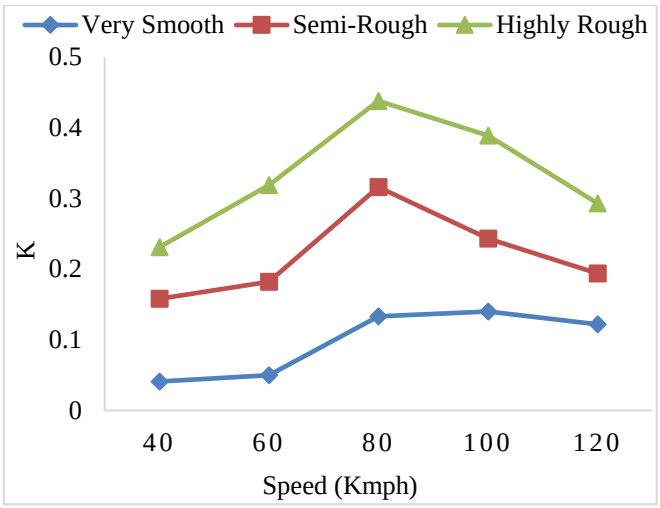

Fig. 10(d) Dieckmann index for trucks moving at the same speed in opposite directions for different road roughness profiles

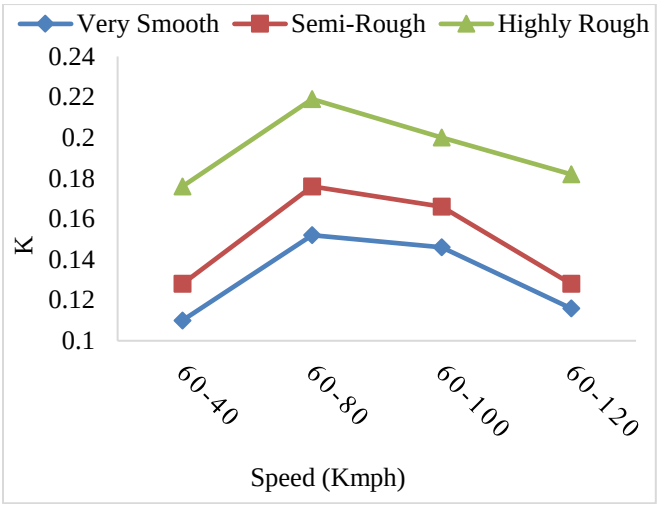

Fig. 10(e) Dieckmann index for trucks moving at a combination of different speeds in the same direction for different road roughness profiles

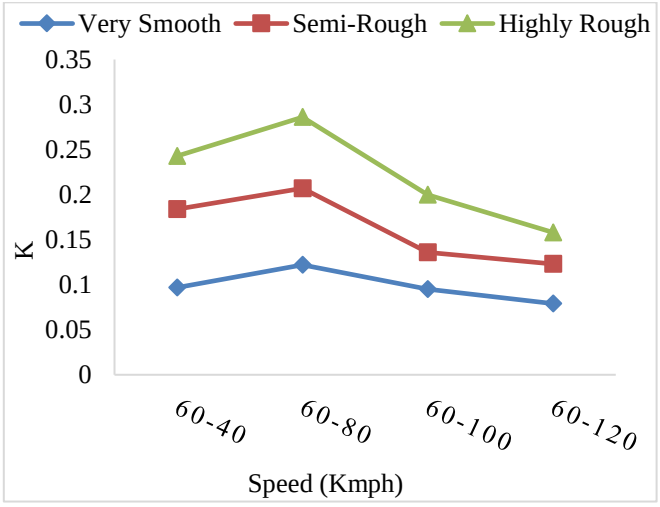

Fig. 10(f) Dieckmann index for trucks moving at a combination of different speeds in opposite directions for different road roughness profiles

A comparison with existing literature highlights that the proposed model outperforms previous studies in terms of accuracy and reliability. While Wang et al. and Zhou et al. [6, 7] reported significant increases in bridge displacement and acceleration with higher vehicle speeds, their models lacked fine-tuned calibration for road roughness variations. In contrast, this study incorporates detailed road roughness classifications based on ISO 8608:2016, allowing for more precise simulations.

The results of the proposed model indicate that for trucks moving at constant speeds, displacement increased by 12%, velocity by 36%, and acceleration by 4%. Unlike Demirlioglu et al. [8], who identified a general trend in dynamic amplification under poor surface conditions, the proposed model provides quantifiable predictions based on varying vehicle speeds and bridge responses.

Furthermore, while Dai et al. [12] observed peak dynamic loads at moderate speeds due to reduced contact duration, the suggested study refines this observation by demonstrating that speeds beyond 80 kmph led to stabilization due to dampening effects in long-span arch bridges. This enhanced level of detail and statistical validation confirms that the current approach offers superior predictive capability, making it a more effective tool for assessing bridge dynamics under real-world loading conditions.

4. Conclusion

The dynamic effect of vehicle loads considering various road roughness conditions on a long-span arch bridge is investigated in the present study. To conduct the vehicle-bridge interaction study, a linear quarter-truck model for the vehicle was established and solved using MATLAB Simulink, and a FEM model of the bridge was developed using midas Civil software. Road profiles for the numerical study were selected following ISO 8608:2016 classification and were developed using MATLAB coding.

Numerical studies were carried out by taking into consideration the effect of speed, direction, and roughness of road profiles under heavy truck loading on the bridge. The dynamic responses of the bridge were extracted and represented in terms of vertical displacements, velocities, and accelerations to locations along the total length of the bridge, as well as the speed of the vehicle on the bridge. The main conclusions drawn from the study are:

The speed of the vehicle has a significant impact on the dynamic response of the bridge. Trucks moving at the same speed have resulted in higher dynamic responses than trucks moving at a combination of different speeds. The crossing time on the bridge, which is directly related to the vehicle speed, affects the dynamic response of the bridge. Also, dynamic responses may not show a linear variation as the speed of the vehicle increases since the dynamic responses are dependent on other factors. The direction of movement of trucks has a substantial effect on the dynamic response of the bridge. Trucks moving in the same direction have led to higher values of dynamic responses, dynamic amplification factor, and Dieckmann index in comparison with trucks moving in opposite directions.

For trucks moving at a combination of different speeds, the combination of 60-80 kmph has resulted in higher dynamic responses, dynamic amplification factor, and Dieckmann index in all the cases, which is because the time taken by the trucks moving at 60 kmph and 80 kmph are comparable. This implies that considering the combination of different speeds on a bridge, the vehicle speeds having comparable crossing times on the bridge are likely to result in higher dynamic responses than any other combination of different speeds.

Among all the combinations considered for the study, trucks moving at the same speed in the same direction have resulted in higher values for the dynamic responses, Dynamic amplification factor, and Dieckmann index. Road roughness plays an important role in the dynamic response of the bridge.

Road surfaces with comparatively fewer undulations resulted in lower values of dynamic responses, which increased further as the degree of roughness of the road increased. The comfort analysis shows that, for the present analyses, the vibrations produced due to the movement of vehicles on the bridge do not adversely affect the comfort level of pedestrians, and the Dieckmann index of comfort analysis for all the cases of loading falls under category 1.

The detailed analysis of the results illustrates that trucks moving at lower speeds in the same direction on a highly rough profile cause more damage to the bridge structure. Therefore, as per the study, maintaining a smooth road surface is of utmost importance to reduce the dynamic effect of vehicle loads on the bridges. Furthermore, the results reveal that it is crucial to consider not only the midspan of the bridge but also adjacent spans, specifically when vehicles are moving in opposite directions.

Therefore, this should be taken into consideration during the analysis and design of long-span bridges. Also, proper inspection and maintenance of bridge elements supporting lanes of traffic moving with lower speeds need to be performed to maintain the service life of the structure. The conclusions drawn from the present study have been adopted for further numerical investigation on the response of the long-span bridge, considering a higher traffic volume on the bridge.

Acknowledgments

The authors thank MIDAS Information Technology Co., Ltd, for providing licensed academic midas Civil 2023 v1.1 software for the research work.

References

[1] M.K. Pant, *Elements of Bridge Engineering*, S.K. Kataria & Sons, pp.1-275, 2014. [Publisher Link]

[2] Eman J. Ismail, "RC Skew Slabs Behaviour: A Finite Element Model," *International Journal of Structural Engineering*, vol. 9, no. 4, pp. 273-288, 2018. [CrossRef] [Google Scholar] [Publisher Link]

[3] Asha Joseph, and Glory Joseph, "Fluid-Structure-Soil Interaction Effect on Dynamic Behaviour of Circular Water Tanks," *International Journal of Structural Engineering*, vol. 10, no. 1, pp. 25-39, 2019. [CrossRef] [Google Scholar] [Publisher Link]

[4] Shrikant M. Harle, "Exploring the Dynamics of Vibration and Impact Loads: A Comprehensive Review," *International Journal of Structural Engineering*, vol. 14, no. 1, pp. 1-24, 2024. [CrossRef] [Google Scholar] [Publisher Link]

[5] Naiwei Lu et al., "Lifetime Deflections of Long-Span Bridges under Dynamic and Growing Traffic Loads," *Journal of Bridge Engineering*, vol. 22, no. 11, 2017. [CrossRef] [Google Scholar] [Publisher Link]

[6] Wei Wang et al., "Dynamic Analysis of a Cable-Stayed Concrete-Filled Steel Tube Arch Bridge under Vehicle Loading," *Journal of Bridge Engineering*, vol. 20, no. 5, 2015. [CrossRef] [Google Scholar] [Publisher Link]

[7] Yufen Zhou, and Suren Chen, "Dynamic Simulation of a Long-Span Bridge-Traffic System Subjected to Combined Service and Extreme Loads," *Journal of Structural Engineering*, vol. 141, no. 9, 2014. [CrossRef] [Google Scholar] [Publisher Link]

[8] Kultigin Demirlioglu, Semih Gonen, and Emrah Erduran, "Effect of Road Roughness on the Dynamic Response of Vehicles in Vehicle-Bridge Interaction Modeling," *Experimental Vibration Analysis for Civil Engineering Structures*, vol. 2, pp. 294-304, 2023. [CrossRef] [Google Scholar] [Publisher Link]

[9] T.G. Konstantakopoulos, I.G. Raftoyiannis, and G.T. Michaltsos, "Suspended Bridges Subjected to Earthquake and Moving Loads," *Engineering Structures*, vol. 45, pp. 223-237, 2012. [CrossRef] [Google Scholar] [Publisher Link]

[10] Yan Zhou, Pengfei Yang, and Kai Zhang, "Dynamic Response Analysis of Cable-Stayed Bridge under Random Traffic Flow and Fleet," *Journal of Vibroengineering*, vol. 23, no. 7, pp. 1663-1679, 2021. [CrossRef] [Google Scholar] [Publisher Link]

[11] Emrah Erduran, Semih Gonen, and Aya Alkanany, "Parametric Analysis of the Dynamic Response of Railway Bridges due to Vibrations Induced by Heavy-Haul Trains," *Structure and Infrastructure Engineering*, vol. 20, no. 3, pp. 326-339, 2022. [CrossRef] [Google Scholar] [Publisher Link]

[12] Li Dai et al., "Effects of Vehicle Speed on Vehicle-Induced Dynamic Behaviors of a Concrete Bridge with Smooth and Rough Road Surfaces," *Applied Sciences*, vol. 13, no. 16, pp. 1-19, 2023. [CrossRef] [Google Scholar] [Publisher Link]

[13] Tao Wang et al., "Wind-Vehicle-Bridge Coupled Vibration Analysis Based on Random Traffic Flow Simulation," *Journal of Traffic and Transportation Engineering (English Edition)*, vol. 1, no. 4, pp. 293-308, 2014. [CrossRef] [Google Scholar] [Publisher Link]

[14] Hai Zhong, Mijia Yang, and Zhili (Jerry) Gao, "Dynamic Responses of Prestressed Bridge and Vehicle through Bridge-Vehicle Interaction Analysis," *Engineering Structures*, vol. 87, pp. 116-125, 2015. [CrossRef] [Google Scholar] [Publisher Link]

[15] M. Agostinacchio, D. Ciampa, and S. Olita, "The Vibrations Induced by Surface Irregularities in Road Pavements - A Matlab® Approach," *European Transport Research Review*, vol. 6, pp. 267-275, 2014. [CrossRef] [Google Scholar] [Publisher Link]

[16] Jianfeng Mao, Zhiwu Yu, and Lizhong Jiang, "Stochastic Analysis of Vehicle-Bridge Coupled Interaction and Uncertainty Bounds of Random Responses in Heavy Haul Railways," *International Journal of Structural Stability and Dynamics*, vol. 9, no. 12, pp. 1-29, 2019. [CrossRef] [Google Scholar] [Publisher Link]

[17] Xuansheng Cheng et al., "Vehicle-Bridge Coupling Dynamic Response of a Box Bridge after Reinforcement with Prestressed CFRP," *Journal of Vibroengineering*, vol. 22, no. 7, pp. 1715-1730, 2020. [CrossRef] [Google Scholar] [Publisher Link]

[18] Hoai Ho, and Mayuko Nishio, "Evaluation of Dynamic Responses of Bridges Considering Traffic Flow and Surface Roughness," *Engineering Structures*, vol. 225, 2020. [CrossRef] [Google Scholar] [Publisher Link]

[19] Fei Xu, Huixian Yang, and Kjell Ahlin, "On Vehicle Response under Non-Gaussian Road Profile Excitation," *Advances in Mechanical Engineering*, vol. 16, no. 4, pp. 1-8, 2024. [CrossRef] [Google Scholar] [Publisher Link]

[20] Giuseppe Loprencipe, and Pablo Zoccali, "Use of Generated Artificial Road Profiles in Road Roughness Evaluation," *Journal of Modern Transportation*, vol. 25, pp. 24-33, 2017. [CrossRef] [Google Scholar] [Publisher Link]

[21] "*ISO 8608:2016-Mechanical Vibration-Road Surface Profiles-Reporting of Measured Data*," ISO, 2016. [Google Scholar] [Publisher Link]

[22] B. Goenaga, L. Fuentes, and O. Mora, "Evaluation of the Methodologies used to Generate Random Pavement Profiles Based on the Power Spectral Density: An Approach Based on the International Roughness Index," *Ingeniería e Investigación*, vol. 37, no. 1, pp. 49-57, 2017. [CrossRef] [Google Scholar]

[23] Chandrashekhar S. Dharankar, Mahesh Kumar Hada, and Sunil Chandel, "Numerical Generation of Road Profile through Spectral Description for Simulation of Vehicle Suspension," *Journal of the Brazilian Society of Mechanical Sciences and Engineering*, vol. 39, pp. 1957-1967, 2017. [CrossRef] [Google Scholar] [Publisher Link]

[24] Luca Rapino et al., "Measurement and Processing of Road Irregularity for Surface Generation and Tyre Dynamics Simulation in NVH Context," *International Journal of Pavement Research and Technology*, vol. 17, pp. 918-928, 2024. [CrossRef] [Google Scholar] [Publisher Link]

[25] Y.B. Yang, Y.C. Lee, and K.C. Chang, *Effect of Road Surface Roughness on Extraction of Bridge Frequencies by Moving Vehicle*, Mechanics and Model-Based Control of Advanced Engineering Systems, Springer, Vienna, pp. 295-305, 2014. [CrossRef] [Google Scholar] [Publisher Link]

[26] Dorra Ben Hassen et al., "Road Profile Estimation Using the Dynamic Responses of the Full Vehicle Model," *Applied Acoustics*, vol. 147, pp. 87-99, 2019. [CrossRef] [Google Scholar] [Publisher Link]

[27] Teron Nguyen et al., "Bus Ride Index - A Refined Approach to Evaluating Road Surface Irregularities," *Road Materials and Pavement Design*, vol. 22, no. 2, pp. 423-443, 2021. [CrossRef] [Google Scholar] [Publisher Link]

[28] Tiago Lima de Sousa, Jéderson da Silva, and Weslen Lins de Araujo, "Optimization of Quarter Car Suspension Dynamics Using Power Spectral Density of Irregular Road Profile," *Universal Journal of Mechanical Engineering*, vol. 11, no. 3, pp. 47-63, 2023. [CrossRef] [Google Scholar] [Publisher Link]

[29] *A Policy on Geometric Design of Highways and Streets*, AASHTO, pp. 1-947, 2001. [Google Scholar] [Publisher Link]

[30] Reza N. Jazar, *Quarter Car Model*, Vehicle Dynamics, Springer, New York, NY, pp. 985-1026, 2014. [CrossRef] [Google Scholar] [Publisher Link]

[31] Majid Pouraminian, and Mohsen Ghaemian, "Shape Optimisation of Concrete Open Spandrel Arch Bridges," *Gradevinar*, vol. 67, no. 12, pp. 1177-1185, 2015. [CrossRef] [Google Scholar] [Publisher Link]

[32] Emadoddin Majdabadi Farahani, and Shahrokh Maalek, "An Investigation of the Seismic Behavior of a Deck-Type Reinforced Concrete Arch Bridge," *Earthquake Engineering and Engineering Vibration*, vol. 16, pp. 609-625, 2017. [CrossRef] [Google Scholar] [Publisher Link]

[33] Yichang Zhang et al., "Vehicle Ride Comfort Analysis Based on Vehicle-Bridge Coupled Vibration," *Shock and Vibration*, vol. 2021, no. 1, pp. 1-14, 2021. [CrossRef] [Google Scholar] [Publisher Link]

[34] IRC: 6-2017, "*Standard Specifications and Code of Practice for Road Bridges, Section: II - Loads and Load Combinations (Seventh Revision)*," Indian Road Congress, pp. 1-122, 2017. [Google Scholar] [Publisher Link]

[35] Jingrui Yang, and Rui Duan, "*Modelling and Simulation of a Bridge Interacting with a Moving Vehicle System*," Master's Degree Thesis, Blekinge Institute of Technology, Karlskrona, Sweden, pp. 1-88, 2013. [Google Scholar]

[36] Fan Feng et al., "Evaluating the Dynamic Response of the Bridge-Vehicle System Considering Random Road Roughness Based on the Moment Method," *Advances in Civil Engineering*, vol. 2021, no. 1, pp. 1-12, 2021. [CrossRef] [Google Scholar] [Publisher Link]

[37] Helu Yu et al., "Road Vehicle-Bridge Interaction Considering Varied Vehicle Speed Based on Convenient Combination of Simulink and ANSYS," *Shock and Vibration*, vol. 2018, no. 1, pp. 1-14, 2018. [CrossRef] [Google Scholar] [Publisher Link]